http://dx.doi.org/10.5935/0100-4042.20150058 *Quim. Nova,* Vol. 38, No. 4, 506-509, 2015

Artigo

METHANE DRY REFORMING OVER Ni SUPPORTED ON PINE SAWDUST ACTIVATED CARBON: EFFECTS OF SUPPORT SURFACE PROPERTIES AND METAL LOADING

Rafael García[a,*], Gabriela Soto[a], Néstor Escalona[a], Catherine Sepúlveda[a], María José Orellana[a], Natalia Morales[a], Ljubisa R. Radovic[b,c], Robison Buitrago-Sierra[d], Francisco Rodriguez-Reinoso[d] and Antonio Sepúlveda-Escribano[d]

[a]Facultad de Ciencias Químicas, Universidad de Concepción, Edmundo Larenas 129, Concepción, Chile

[b]Facultad de Ingeniería, Universidad de Concepción, Edmundo Larenas 215, Concepción, Chile

[c]Department of Energy and Mineral Engineering, Penn State University, Pennsylvania, USA

[d]Laboratorio de Materiales Avanzados, Departamento de Química Inorgánica, Universidad de Alicante, Alicante, España

Recebido em 13/10/2014; aceito em 16/01/2015; publicado na web em 14/04/2015

The influence of metal loading and support surface functional groups (SFG) on methane dry reforming (MDR) over Ni catalysts supported on pine-sawdust derived activated carbon were studied. Using pine sawdust as the catalyst support precursor, the smallest variety and lowest concentration of SFG led to best Ni dispersion and highest catalytic activity, which increased with Ni loading up to 3 Ni atoms nm^{-2}. At higher Ni loading, the formation of large metal aggregates was observed, consistent with a lower "apparent" surface area and a decrease in catalytic activity. The H_2/CO ratio rose with increasing reaction temperature, indicating that increasingly important side reactions were taking place in addition to MDR.

Keywords: methane dry reforming; Ni/activated carbons catalysts; support surface functional group influence.

INTRODUCTION

Combined conversion and utilization of carbon dioxide and methane presents important practical and fundamental challenges in C1 chemistry. Conversion of CH_4 requires consumption of oxygen, while that of CO_2 requires hydrogen. So, their simultaneous conversion is in principle an ideal application of oxidation/reduction reactions. Of special interest is CO_2 activation for its efficient removal and conversion to higher-value-added products, as well as the methane dry reforming (MDR) using Ni catalysts, in order to obtain synthesis gas for subsequent production of methanol or Fischer-Tropsch synthesis.[1-11]

Wang *et al.* presented the state of the art in MDR and discussed the thermodynamics of CH_4/CO_2 reaction, as well as the main side reactions.[12] One of their conclusions was related to selection of the active phase and support, and the effect of their interaction on catalytic activity.

However, there exists scant literature on the use of activated carbon (AC) as support in MDR. Matos *et al.* used a commercial support but only reported its surface area.[13] Ferreira-Aparicio *et al.* studied the addition of MgO to a ruthenium catalyst dispersed on a commercial AC and again only textural characterization was reported.[14] Bradford and Vannice did examine the support influence on catalytic activity and carbon deposition; they concluded that the activity of a Ni/C catalyst was very similar to that of a Ni/SiO_2 catalyst.[15] Similarly, Wu *et al.* reported a relatively high activity of a Co/C catalyst.[16] Song *et al.* used both an AC and a coal char as catalysts and reported a higher activity of the former, due to its higher surface area; they also mentioned that the surface functional groups may account for the higher catalytic activity. [17]

Based on this representative summary of the literature on MDR using AC as support, it is clear that there is much uncertainty regarding the relative importance of support's textural and chemical surface properties. Furthermore, the AC support's durability under reaction conditions (i.e., high temperature and CO_2 atmosphere) is hardly ever reported. Here we provide such information using Ni catalysts supported on characterized activated carbons; in particular, we examined how the AC's surface functional groups and Ni loading affect catalytic activity and the resulting H_2/CO ratio.

*e-mail: rgarcia@udec.cl

EXPERIMENTAL

Preparation of supports and catalysts

The PSAC was prepared by chemical activation of pine sawdust, using H_3PO_4 (4 mol L^{-1}) at 25 ºC during 72 h, followed by 100 mL min^{-1} of N_2 flow at 450 °C for 4 h. The solid was thoroughly washed until complete removal of residual phosphorus compounds. Removal of residual surface functionaleties was achieved by heat treatment in He (100 mL min^{-1}) at 1000 °C (PSAC-He).

The AC-supported nickel catalysts were prepared by incipient wetness impregnation of PSAC and PSAC-He using $Ni(NO_3)_2{\cdot}6H_2O$. These samples were dried overnight at 105 °C, calcined at 200 °C for 12 h, reduced *in situ* at 450 °C using 50 mL min^{-1} of H_2 flow for 3 h and finally stabilized with 50 mL min^{-1} of Ar flow at 950 ºC. Four catalysts were prepared with the PSAC-He support, containing 1, 2, 3 and 4 Ni atoms per nm^2 of support (Ni(1)/PSAC-He, Ni(2)/PSAC-He Ni(3)/PSAC-He and Ni(4)/PSAC-He), as well as a catalyst containing 3 Ni atoms nm^{-2} on PSAC (Ni(3)/PSAC).

Characterization of supports and catalysts

The "apparent" BET surface area (S_{BET}) of the supports and catalysts was determined from N_2 adsorption isotherms at 77 K (Micromeritics Tristar II 3020 volumetric apparatus). Surface functional groups (SFG) on the support were determined by temperature-programmed decomposition (TPD) in an apparatus having a thermal conductivity detector coupled to a non-dispersive infrared (NDIR) analyzer. TPD analysis was carried out using 0.1 g of dry solid in He flow (50 mL min^{-1}) up to 1050 ºC with 18 ºC min^{-1} of heating rate. The precursors and the catalysts were analyzed by Temperature programmed reduction (TPR), using a flow (50 mL min^{-1}) of H_2 (5%)/Ar mixture from 25 up to 1050 ºC with 10 ºC min^{-1} of heating

rate. X-ray photoelectron spectroscopy (XPS, Multilab Microtech VG-300 system) was used for complementary characterization of surface oxygen groups and as an estimate of Ni dispersion, using the Ni/C atomic ratio. Metal particle size distribution (PSD) of the catalyst, dispersed in acetone, was obtained by transmission electron microscopy (TEM) (JEOL TEM 2010).

Catalytic activity tests

Catalytic activity was measured in a continuous-flow fixed-bed quartz microreactor, using approximately 22 mg of catalyst (stabilized at 950 ºC under Ar flow) contacted with 60 mL min^{-1} of reactant gas mixture (1:1 CH_4/CO_2). The catalysts were previously reduced in situ in H_2 flow (12 mL min^{-1}) during 3 h at 450 ºC. According to the literature, diffusional limitations are minimized under these experimental conditions.[15] Methane conversion first-order rate constants (k) are calculated from the reactor design equation applied to a fixed-bed continuous-flow reactor. The assumption first-order is supported by Song *et al.* and Özkara-Aydınoglu *et al.*.[17,18] The concentrations of CH_4, CO_2, CO and H_2 were monitored at the reactor outlet by on-line gas chromatography (TCD), using a 4.6 m Carboxen-1000 (60/80) packed column.

RESULTS AND DISCUSSION

Characterization of supports and catalysts

Nitrogen adsorption (not shown) of all catalysts displayed a Type I adsorption isotherm characteristic of microporous solids. The PSAC thermal treatment in He decreased its S_{BET} from 1170 to 986 $m^2 g^{-1}$. Table 1 shows corrected S_{BET} by the dilution effect due to the higher Ni content on activated carbon. There is a gradual decrease in S_{BET} upon Ni addition to PSAC-He support; this is attributed to micropore blocking at the higher Ni loadings.

Table 1. Summary of XPS results and "apparent" surface area of the catalysts

Catalyst	Ni $2p_{3/2}$ (eV)	Ni/C (at at^{-1})	S_{BET} ($m^2 g^{-1}$)
Ni(3)/PSAC	852.9 (64) 856.4 (36)	0.037	703
Ni(1)/PSAC-He	852.9 (94) 855.7 (6)	0.011	650
Ni(2)/PSAC-He	852.9 (85) 854.8 (15)	0.017	633
Ni(3)/PSAC-He	852.9 (84) 855.7 (16)	0.076	630
Ni(4)/PSAC-He	852.6 (84) 855.9 (16)	0.053	582

TPR profile of precursors (not show here) displayed a principal reduction peak centered on 350 ºC, it correspond to reductive decomposition of the Ni precursor. This temperature value is related with weak interaction between precursor and support.[19] From this result and bibliography the temperature used to obtain the reduced Ni supported catalysts was 450 ºC.[20,21] Using this reduction procedure, any reduction peak was observed in the TPR profile for reduced catalysts.

The TEM micrographs show these particles (Figures 1 and 2); furthermore, thermal treatment of the support is seen (Figure 1) to promote a more homogeneous dispersion of the metallic phase. The particle size distribution of Ni in Ni(3)/PSAC-He catalyst (Figure 1b) was 15-60 nm, centered at 50 nm; in contrast, Ni(3)/PSAC catalyst formed larger Ni agglomerates (ca. 80 nm) as well as smaller particles (ca. 15 nm). As metal loading increased, there was a wider catalyst PSD (Figure 2); indeed, at highest Ni loading, the Ni agglomerates had an average particle size closer to 500 nm.

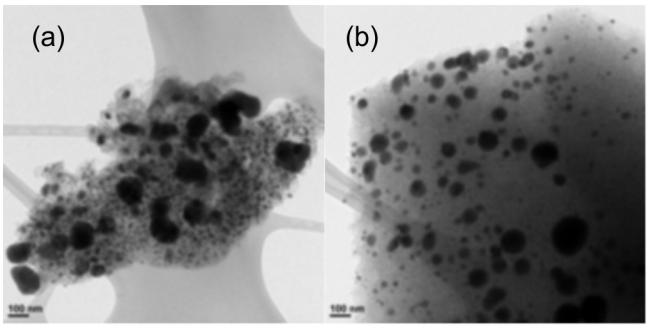

Figure 1. *TEM micrographs of Ni(3)/PSAC (a) and Ni(3)/PSAC-He (b) catalysts*

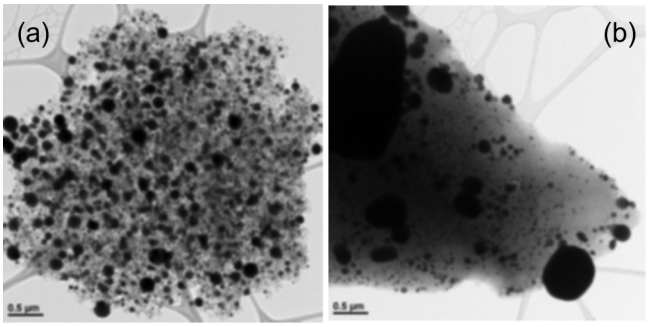

Figure 2. *TEM micrographs of Ni(3)/PSAC-He (a) and Ni(4)/PSAC-He (b) catalysts*

Figure 3 illustrates the significant decrease in SFG after heat treatment of the support. Abundant literature on this subject provides the means to characterize this process, according to temperature and identification of evolved gases (mainly CO/CO_2).[22-24] The original support TPD profile shows CO_2 evolution (detected by NDIR) between 200 and 250 °C, corresponding to decomposition of carboxylic acid groups. The broad gas evolution that starts near 400 °C is evidence for the presence of lactonic groups. As temperature increases (700-900 ºC), CO_2 evolution decreases and the evolution of CO simultaneously increases, which is evidence for the presence of anhydride, phenolic and quinone groups. The TPD profile of sample PSAC-He only shows a small CO peak centered near 900 °C, which is assigned to pyrone and/or quinone groups. In summary, and as expected, the

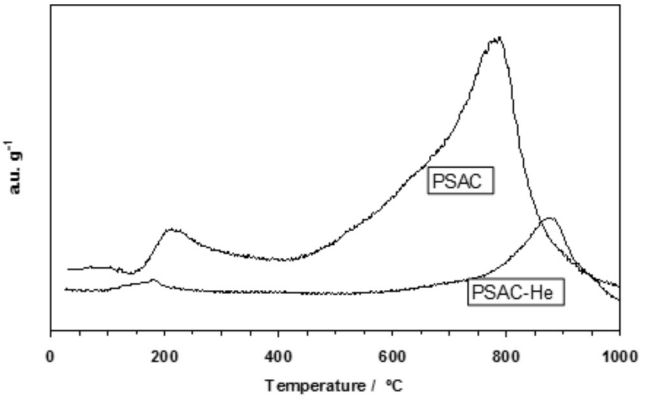

Figure 3. *Temperature-programmed decomposition (TPD) profiles for PSAC and PSAC-He supports*

PSAC support has a much greater variety and a higher concentration of oxygen SFG than its thermally treated counterpart.

The XPS results (profile not shown hear), for Ni/PSAC catalysts displayed mainly three contributions in O_{1S} region, quinone at 531.5 eV (40%), anhydride at 533.4 eV (41%) and chemisorbed water at 535.5 eV (19%). In the Ni/PSAC-He catalyst, the XPS shows that chemisorbed water is absent due to thermal treatment, the quinone groups enhance their contribution at 57 %, the anhydride diminished up to 27 % and a new contribution appears at 530.2 eV, attributed to C=O of carbonyl groups.[25,26]

The chemical state and the relative amounts of surface nickel in the reduced catalysts were determined by XPS (Table 1). The primary Ni $2p_{3/2}$ component was fixed at about 852.9 eV for all samples, and it can be assigned to the reduced Ni species. A second Ni $3p_{3/2}$ peak at about 855.7 eV is attributed to oxidized Ni species.[27] Based on relative intensities, the Ni(3)/PSAC-He catalyst has a more reduced Ni surface than the Ni(3)/PSAC catalyst. Also, the Ni/C atomic ratios indicate a higher Ni dispersion for the Ni(3)/PSAC-He catalyst, in agreement with TEM results (Figure 1). Thus, surface cleaning of the AC support favors higher metal dispersion, and the smaller Ni particles are more easily reduced. These results suggest that SFG, which decomposed at lower temperatures, are responsible for strong interaction between the Ni and PSAC support and thus decrease reducibility and dispersion. Finally, Table 1 shows that Ni/C atomic ratio increases with increasing Ni content up to 3 Ni atoms nm^{-2}, and then it decreases. This is attributed to formation of Ni particles aggregates over the support, and is supported by the TEM results shown in Figure 2.

CATALYTIC ACTIVITY

All catalysts tested displayed a catalytic reaction stability of at least eight hours on-stream. This behavior suggests that coke deposition on catalysts would not produce in agreement with the values of textural properties obtained after reaction and in according to the previously reported by Scaroni *et al.*.[28] So, the support obtained by chemical activation of pine sawdust using H_3PO_4, is indeed a promising one for commercial applications. During the catalytic test only H_2, O_2, CO, CO_2 and CH_4 were quantitatively detected. The absence of water peak in the chromatograms can not discard the possible formation of water by the reverse water gas shift (RWGS) reaction. The water formed by RWGS can be consumed in situ by other side reactions, such as, the methane steam reforming reaction.

The Ni(3)/PSAC-He catalyst was more active than Ni(3)/PSAC (Table 2) at all temperatures studied. As evidenced by both XPS and TEM results, this is a consequence of its higher reduced metallic Ni proportion and higher Ni dispersion. This is in agreement with the study of Fidalgo *et al.*, who reported that catalysts prepared with an oxidized carbon support had a lower metal dispersion and were less active.[29] However, these authors did not pay attention to the chemical surface characteristics of the activated carbon supports, such as suggest by Radovic and Rodriguez-Reinoso and its validity is confirmed in the present study.[30]

Table 2 shows that the H_2/CO ratio is less than 1 in all cases. Choudhary and Mondal reported similar results, and attributed them to the reverse water gas shift (RWGS) reaction.[31] In our case the H_2/CO ratio increases up to 0.83 as the reaction temperature increased. Such trend has been reported previously and was attributed to several side reactions that can take place, together with MDR, at higher temperatures:[12,15,31,32,33]

i) RWGS reaction,

$$CO_2 + H_2 \leftrightarrows H_2O + CO \quad (1)$$

ii) Boudouard reaction,

$$2CO \leftrightarrows CO_2 + C \quad (2)$$

iii) methane cracking reaction,

$$CH_4 \leftrightarrows C + 2H_2 \quad (3)$$

iv) Methane steam reforming reaction (MSR)

$$CH_4 + H_2O \leftrightarrows CO + 3H_2 \quad (4)$$

The Table 2 summarized the overall activation energy values obtained from Arrhenius plot. These values, higher than 100 kJ mol^{-1}, are similar to those reported by Bradford and Vannice for a 6.3 wt.% Ni/C catalyst (121 kJ mol^{-1}) and by Song *et al.* who used coal-derived commercial AC catalysts (136 kJ mol^{-1}).[34,17] These relatively high values of activation energy, together with the high space velocity (GHSV around 6000 h^{-1}) used, suggest that diffusional limitations are minimized, and thus the chemical characteristics of the catalytic reaction are dominant.

In the Ni(X)/PSAC-He catalysts, as can be seen in Figure 5, the most active is Ni(3)/PSAC-He and its activation energy is the highest. This behavior is attributed to the often observed compensation effect, as shown in Figure 4.[35-37] The isokinetic temperature obtained from this plot is 624 ºC, lower than the reaction temperatures confirming that the more active catalyst should have the higher apparent activation energy. It should be noted that experimental error in the Arrhenius plots or a change in reaction mechanism, could give rise to a false ''apparent'' compensation effect.[37]

Table 2. Effect of reaction temperature on pseudo first-order rate constant (k), H_2/CO ratio and activation energy (E_a) values for Ni(3)/PSAC and Ni(X)/PSAC-He series catalysts

Catalysts	Temperature (°C)	k (h^{-1})	H_2/CO	E_a (kJ mol^{-1})
Ni(3)/PSAC	750	0.172	0.578	115
	800	0.221	0.699	
	900	0.909	0.816	
Ni(1)/PSAC-He	750	0.085	0.530	104
	800	0.154	0.534	
	900	0.406	0.668	
Ni(2)/PSAC-He	750	0.222	0.503	112
	800	0.316	0.509	
	900	1.153	0.764	
Ni(3)/PSAC-He	750	0.270	0.521	151
	800	0.461	0.583	
	900	2.501	0.801	
Ni(4)/PSAC-He	750	0.120	0.531	109
	800	0.184	0.552	
	900	0.600	0.784	

Figure 5 summarizes the behaviour of Ni(x)/PSAC-He catalysts. Activity increases with loading up to 3 Ni atoms nm^{-2}, and then decreases. The increase is attributed to a higher concentration of active sites (higher Ni dispersion), as evidenced by XPS results. The activity loss for sample Ni(4)/PSAC-He is attributed to loss of dispersion as a consequence of the formation of large Ni aggregates, as evidenced by TEM, and in agreement with the abrupt decrease in catalyst surface area in comparison to catalysts with lower Ni content. Although the Ni/C atomic ratio of this catalyst (Table 1) is higher

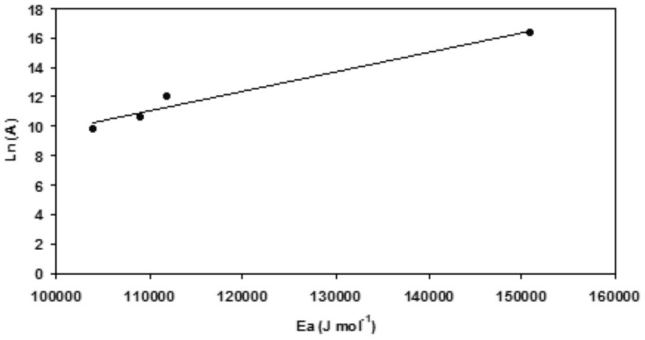

Figure 4. *Compensation effect plot for Ni(X)/PSAC-He catalysts series*

than Ni(1)/PSAC-He and Ni(2)/PSAC-He catalysts, it has to be taken into account that at this high Ni loading, the Ni/C value by XPS measurements may be overestimated. This behaviour was probably due to the formation of large Ni clusters on the external surface of support, which reduce disproportionately the exposed carbon surface. The large activity increase with Ni loading at 900 ºC is in agreement with the higher spontaneity of MDR and methane cracking reactions at this temperature.

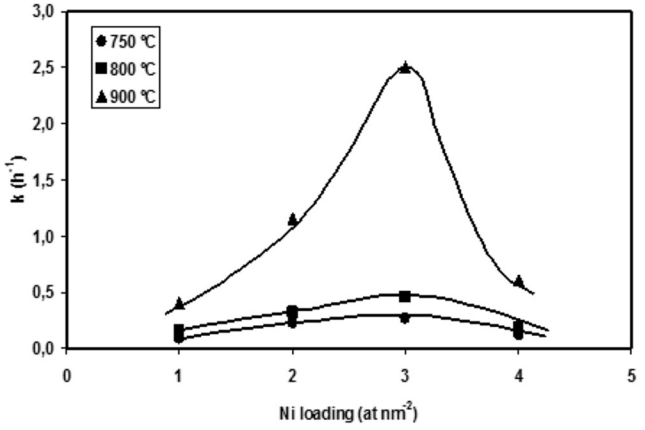

Figure 5. *Effect of metal loading on the activity of Ni(x)/PSAC-He catalysts*

CONCLUSIONS

The preparation of carbon support by chemical activation of pine sawdust using H_3PO_4, led to stable catalysts under MDR reaction conditions. The detrimental effect of SFG on the support was demonstrated. Using this activated carbon support, the smallest variety and lowest concentration of SFG promote high Ni dispersion and high catalytic activity, which increases with Ni content up to 3 Ni atoms per nm^2 of support. The decrease in catalytic activity above this loading is attributed to the formation of large metal aggregates, resulting in pore blocking and lower catalyst surface area.

ACKNOWLEDGEMENTS

Financial support was provided by CONICYT PFB-27 project (UDT-University of Concepción) and FONDECYT 1100884 grant.

REFERENCES

1. Sugino, M.; Shimada, H.; Turuda, T.; Miura, H.; Ikenaga, N.; Suzuki, T.; *Appl. Catal., A* **1995**, *121*, 125.
2. Huang, W.; Xie, K. C.; Wang, J. P.; Gao, Z. H.; Yin, L. H.; Zhu, Q. M.; *J. Catal.* **2001**, *201*, 100.
3. Rezaei, M.; Alavi, S. M.; Sahebdelfar, S.; Yan, Z. F.; *Scr. Mater.* **2009**, *61*, 173.
4. Wu, J. C. S.; Chou, H. C.; *Chem. Eng. J.* **2009**, *148*, 539.
5. Liu, D.; Lau, R.; Borgna, A.; Yang, Y.; *Appl. Catal., A* **2009**, *358*, 110.
6. Wang, S.; Lu, G. Q. M.; *Appl. Catal., B* **1998**, *16*, 269.
7. Lemonidou, A. A.; Vasalos, I. A.; *Appl. Catal., A* **2002**, *228*, 227.
8. Lee, S. H.; Cho, W.; Ju, W. S.; Cho, B. H.; Lee, Y. C.; Baek, Y. S.; *Catal. Today* **2003**, *87*, 133.
9. Halliche, D.; Bouarab, R.; Cherifi, O.; Bettahar, M. M.; *Catal. Today* **1996**, *29*, 373.
10. Tomishige, K.; Yamazaki, O.; Chen, Y.; Yokoyama, K.; Li, X.; Fujimoto, K.; *Catal. Today* **1998**, *45*, 35.
11. Hong, S. W.; Oh, S. M.; Park, D. W.; Kim, G. J.; *J. Ind. Eng. Chem.* **2001**, *7*, 410.
12. Wang, S.; Lu, G. Q. M.; Millar, G. J.; *Energy Fuels* **1996**, *10*, 896.
13. Matos, J.; Diaz, K.; Garcia, V.; Cordero, T. C.; Brito, J. L.; *Catal. Lett.* **2006**, *109*, 163.
14. Schuurman, Y.; Mirodatos, C.; Ferreira-Aparicio, P.; Rodríguez-Ramos, I.; Guerrero-Ruiz, A.; *Catal. Lett.* **2000**, *66*, 33.
15. Bradford, M. C. J.; Vannice, M. A.; *Appl. Catal., A* **1996**, *142*, 73.
16. Wu, Y.; Osamu, K.; Tsuneo, M.; *J. Jpn. Pet. Inst.* **1999**, *42*, 86.
17. Song, Q.; Xiao, R.; Li, Y.; Shen, L.; *Ind. Eng. Chem. Res.* **2008**, *47*, 4349.
18. Özkara-Aydınoglu, S., Aksoylu, A. E.; *Chem. Eng. J.* **2013**, *215*, 542.
19. Yaakob, Z.; Bshish, A.; Ebshish, A.; Tasirin, S. M.; Alhasan, F. H.; *Materials* **2013**, 6, 2229.
20. Fidalgo, B.; Zubizarreta, L.; Bermúdez, J. M.; Arenillas, A.; Menéndez, J. A.; *Fuel Process. Technol.* **2010**, 91, 765.
21. Liu, Y.; Chen, J.; Zhang, J.; *Chin. J. Chem. Eng.* **2007**, *15*, 63.
22. Domingo-García, M.; Lopez Garzon, F. J.; Pérez-Mendoza, M. J.; *J. Coll. Int. Sci.* **2002**, *248*, 116.
23. Figueiredo, J. L.; Pereira, M. F. R.; Freitas, M. M. A.; Órfão J. J. M.; *Carbon* **1999**, *37*, 1379.
24. Halttunen M. E.; Niemelä, M. K.; Krause, A. O. I.; Vaara, T.; Vuori, A. I.; *Appl. Catal., A* **2001**, *205*, 37.
25. Rosenthal, D.; Ruta, M.; Schlögl, R.; Kiwi-Minsker, L.; *Carbon* **2010**, *48*, 1835.
26. Valdes, H.; Sanchez-Polo, M.; Rivera-Utrilla, J.; Zaror, C. A.; *Langmuir* **2002**, *18*, 2111.
27. Czekaj, I.; Loviat, F.; Raimondi, F.; Wambach, J.; Biollaz, S.; Wokaun, A.; *Appl. Catal., A* **2007**, *329*, 68.
28. Scaroni, A. W.; Jenkins, R. G.; Walker Jr., R. G.; *Appl. Catal., A* **1985**, *14*, 173.
29. Fidalgo, B.; Zubizarreta, L.; Bermúdez, J. M.; Arenillas, A.; Menéndez, J. A.; *Fuel Process. Technol.* **2010**, *91*, 765.
30. Radovic, L. R.; Rodríguez-Reinoso, F.; In *Chemistry and Physics of Carbon, vol. 25*; Thrower, P. A., ed.; Marcel Dekker, New York: 1997, pp. 243-358.
31. Choudhary, V. R.; Mondal, K. C.; *Appl. Energy* **2006**, *83*, 1024.
32. Ferreira-Aparicio, P.; Marquez-Alvarez, C.; Rodrıguez-Ramos, I.; Schuurman, Y.; Guerrero-Ruiz, A.; Mirodatos, C.; *J. Catal.* **1999**, *184*, 202.
33. Choudhary, V. R.; Rajput, A. M.; *Ind. Eng. Chem. Res.* **1996**, *35*, 3934.
34. Bradford, M. C. J.; Vannice, M. A.; *Appl. Catal., A* **1996**, *142*, 97.
35. Baeza, P.; Ojeda, J.; Escalona, N.; Alvez, G.; García, R.; Cid, R.; Gil Llambías, F. J.; *Bol. Soc. Chil. Quím.* **2001**, *46*, 415.
36. Bennett, C. A.; Kistler, R. S.; Nangia, K.; Al-Ghawas, W.; Al-Hajji, N.; Al-Jemaz, A.; *Proceedings of 7th International Conference on Heat Exchanger Fouling and Cleaning - Challenges and Opportunities*, Tomar, Portugal, **2007**.
37. Bond, G. C.; Keane, M. A.; Kral, H.; Lercher, J. A.; *Catal. Rev.* **2000**, *42*, 323.